

## **CHARACTERISATION OF THE NANOTUBULAR OXIDE LAYER FORMED ON THE ULTRAFINE-GRAINED TITANIUM**

*Dragana R. Barjaktarević<sup>\*1</sup>, Marko P. Rakin<sup>1</sup>, Veljko R. Djokić<sup>2</sup>*

<sup>1</sup>*Faculty of Technology and Metallurgy, University of Belgrade,  
Karnegijeva 4 11120 Belgrade, Serbia*

<sup>2</sup>*Innovation Centre of the Faculty of Technology and Metallurgy,  
University of Belgrade, Karnegijeva 4 11120 Belgrade, Serbia*

*Received 03.12.2018.*

*Accepted 17.12.2018.*

### **Abstract**

Commercially pure titanium (cpTi) and titanium alloys are metallic implant materials usually used in dentistry and orthopaedics. In order to improve implant properties, Ti-based materials may be surface modified by different procedures. One of the most attractive methods is electrochemical anodization, as a method for obtaining nanotubular oxide layer on the material surface, aiming at improving mechanical, biological and corrosion properties of the metallic biomaterials. In the present study, ultrafine-grained titanium (UFG cpTi) was obtained by high pressure torsion (HPT) under a pressure of 4.1 GPa with a rotational speed of 0.2 rpm, up to 5 rotations at room temperature. In order to form homogeneous nanotubular oxide layer on the UFG cpTi, the electrochemical anodization was performed in phosphoric acid containing 0.5 wt. % of NaF electrolyte during anodizing times of 30, 60 and 90 minutes. The characterisation of thus formed nanotubes was performed using the scanning electron microscopy (SEM), while the surface topography was analysed using the atomic force microscopy (AFM). The results show that the electrochemical anodization process leads to an enhanced roughness of the surface. The mechanical behaviour of the UFG cpTi after the electrochemical anodization process is estimated using the nanoindentation technique. Obtained results show that anodized material has lower value of nanohardness than non-anodized material. Moreover, anodized UFG cpTi has lower modulus of elasticity than non-anodized UFG cpTi and the value is close to those observed in bones.

**Key words:** electrochemical anodization; high pressure torsion; nanotubular oxide layer; ultrafine-grained titanium

---

\* Corresponding author: Dragana R. Barjaktarević, [dbarjaktarevic@tmf.bg.ac.rs](mailto:dbarjaktarevic@tmf.bg.ac.rs)

## Introduction

Titanium based materials are one of the frequently used metallic biomaterials in dentistry and orthopaedics [1]. These materials have become materials of choice due to their favourable characteristics, such as corrosion resistance, osseointegration and biocompatibility in the human body environment [2-4]. Young's modulus is one of the major factors in the selection of metallic biomaterials, and its value should be equivalent to that of the bone in order to make the bone and implant closer by properties [5].

It was shown that nanostructuring of the commercially pure titanium (cpTi) using severe plastic deformation (SPD) leads to a better mechanical properties and biological response [6, 7]. High pressure torsion (HPT) is efficient SPD method for production of ultrafine-grained (UFG) materials with grain size in the range from 100 nm to 500 nm [8]. The HPT process is performed by machine with two anvils, and the sample in the shape of a disk with small dimension is placed between them. The disk is subjected to high pressure, while shear strain is induced in the disk by rotation of the anvils in opposite directions [9]. The HPT process is illustrated in Fig. 1. The equation (1) shows that the shear strain value during HPT process is zero in the centre and becomes maximum at the edge of the disk [7].

$$\gamma = 2\pi NR / h \quad 1$$

In the equation,  $N$  is the number of revolutions,  $R$  is the radial distance from the disk centre and  $h$  is the disk thickness. The equation (1) describes the influence of the HPT process on the microstructure of the material, indicating that the centre of the disk after HPT process has lower change in grain refinement than the edge of the disk [9].

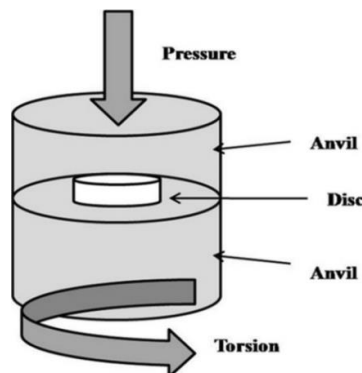


Fig. 1. The high pressure torsion process.

In recent years, electrochemical anodization has been widely used to form the nanostructured titanium surface in order to improve biomaterials surface properties. This nanostructured surface modification method allows the formation of an oxide layer much thicker than the natural oxide layer formed on the titanium surface [10]. In the electrochemical anodization process, electrolyte with fluoride ions leads to the formation of nanotubular oxide layers [11], while compact oxide layers can be formed in most electrolytes, as presented in Fig. 2.

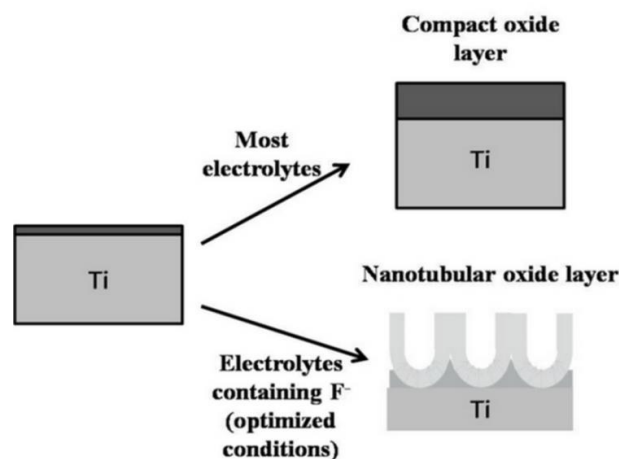


Fig. 2. Formation of the oxide layer on the titanium surface.

The nanotubular oxide layer formed on the titanium and its alloy has  $\text{TiO}_2$  based nanotubes with various diameters ranging from 15 to 300 nm [12]. Their morphology depends on the electrochemical anodization parameters. Different dimension of nanotubes could be created by varying electrolyte, its pH values and concentration, voltage and anodizing time. By increasing anodizing time, the thickness of the nanotubular oxide layer can increase as well. It was shown that increasing the anodizing time from 5 minute to 480 minutes leads to an increase of nanotubes length up to 22  $\mu\text{m}$ , in the case of Ti-28Nb-28Zr alloy [13]. The anodization processing of cpTi in the time range from 15 minutes to 120 minutes leads to the formation of a nanotubular oxide layer with limited thickness of about 2  $\mu\text{m}$  after 120 minutes [14]. However, increasing anodizing time leads to decreasing the thickness of the nanotube wall [15]. The nanotubular oxide layers formed on the titanium-based materials are compiled of the elements in the base material. For instance, nanotubular oxide layer formed on the Ti-Al alloy is composed of  $\text{TiO}_2$  and  $\text{Al}_2\text{O}_3$ . The amounts of these oxides in the nanotubular oxide layer are proportional to the amounts of Ti and Al elements in base alloys [16]. Nanotubular oxide layer formed on the cpTi is composed of a combination of Ti oxides, mainly of  $\text{TiO}_2$  and  $\text{Ti}_2\text{O}_3$  oxides.

The formation of nanotubular oxide layer on the titanium surface leads to improvement of the corrosion resistance, biocompatibility and osseointegration, reduces modulus of elasticity and approaches to that of the human bone [12]. Due to these properties and possibilities of their modifications, the cpTi and titanium alloys are now extensively used to fabricate biomedical devices, such as cardiovascular stents, spinal fixation devices, screws, dental implants.

In the present study, the nanotubular oxide layer formation on the ultrafine-grained titanium in an electrolyte with fluoride ions, during different anodizing times was examined, aiming at analysing the morphology, mechanical and chemical properties of the nanotubular surface.

## Materials and Methods

The cpTi sample was a disc with a diameter of the 28 mm and thickness of 2.26 mm. Chemical composition of the cpTi is given in Table 1.

Table 1. Chemical composition of cpTi (% weight)

| C    | H     | N    | O    | F    | Ti     |
|------|-------|------|------|------|--------|
| 0.10 | 0.015 | 0.03 | 0.25 | 0.30 | 99.305 |

The cpTi was subjected to the high-pressure torsion (HPT) at the pressure of 4.1 GPa and speed of 0.2 rpm in 5 revolutions. After HPT process, the ultrafine-grained titanium (UFG cpTi) was obtained. The sample of UFG cpTi was a disc with a diameter of 34 mm and thickness of approximately 1.37 mm. These obtained samples were polished with carbide paper in the range from 100 to 4000, cleaned with acetone and ethanol and then rinsed with distilled water.

## Electrochemical anodization

The equipment for electrochemical anodization process consists of two electrodes: samples before and after anodization process as the anode and platinum as the counter electrode. DC power source (PEQLAB EV 231) was used for the anodization process. The anodization process was realised during the anodizing time in the range between 30 minutes to 90 minutes in 1M H<sub>3</sub>PO<sub>4</sub> + 0.5 wt. % NaF, using a set potential of 25 V. Current density is one of the parameters of anodization process, which changes during the time. The changing of current density is shown in Fig. 3.

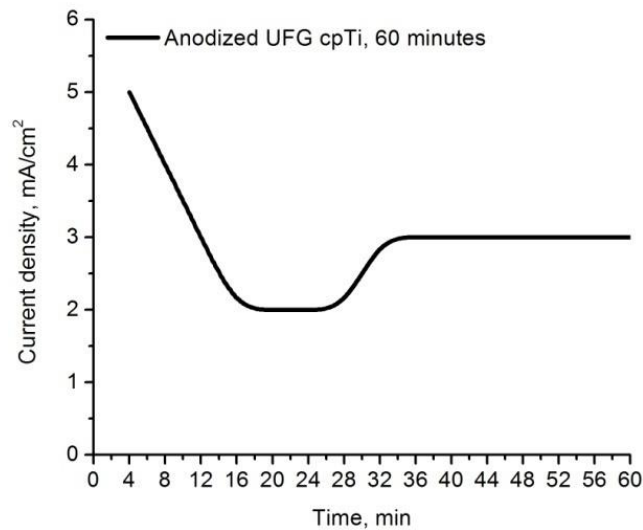


Fig. 3. Schematic drawing of changing in current density during anodization process.

Scanning electron Microscopy (FEG-SEM) TESCAN MIRA3 was used for characterisation of anodized surface, while chemical composition of the nanotubular

oxide layer was determined using Scanning Electron Microscopy (Jeol5800) with Energy Dispersive Spectroscopy (EDS).

### Surface characterisation by Atomic Force Microscopy (AFM)

Surface topography of the samples was analysed by Atomic Force Microscopy (AFM, Veeco – Nanoscope III d) in the tapping mode with a tip, which had a height of 10-12  $\mu\text{m}$  and a tip radius of 10 nm. AFM measurements were done in ambient condition.

### Mechanical characterisation

The nanoindentation test was performed on the sample surface using the Nanoindenter G200, Agilent Technologies. Total displacement of 2000 nm for non-anodized sample and total displacement of 300 nm (10% of the thickness of nanotubular oxide layer) for anodized sample were used. The determination of the properties of the thin layer using nanoindentation technique is carried out at maximal displacement of 10% of the layer thickness [17]. Mean value of ten measurements for each sample was calculated. The nanoindentation test was applied to evaluate the mechanical properties of the surface after the electrochemical anodization.

## Results and discussion

### *The morphology of nanotubular oxide layer*

The morphologies of the nanotubular oxide layer on the UFG cpTi surface formed during anodizing times of 30, 60 and 90 minutes are shown in Fig. 4. As can be seen in the SEM images, only the anodization process after 60 minutes led to the formation of a nanotubular oxide layer Fig. 4 (b). The nanotubes had an average diameter of 100 nm, while the thicknesses of the nanotube walls were approximately 30 nm. Nanotubes were open on the top and their average length is approximately 3  $\mu\text{m}$ . The obtained image clearly demonstrates that anodization of titanium in an electrolyte with fluoride ions could lead to the formation of the nanotubular oxide layer. On the contrary, the anodization process after 30 and 90 minutes did not lead to the formation of a nanotubular oxide layer. It could be concluded that an anodizing time of 30 minutes was not enough to form nanotubes Fig. 4 (a), while an anodizing time of 90 minutes led to the decomposition of the already formed nanotubular oxide layer Fig. 4 (c).

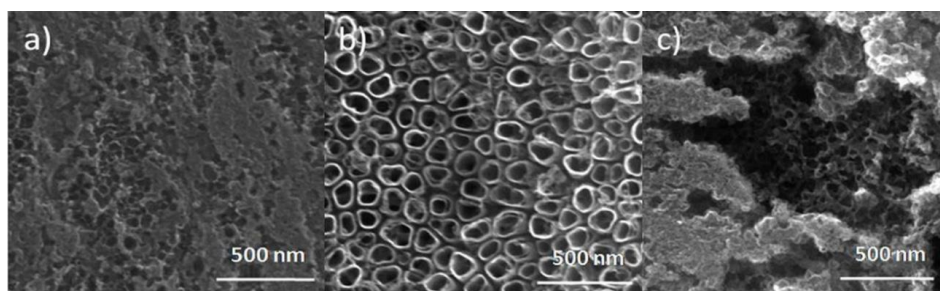


Fig. 4. Nanotubular oxide layer on the UFG cpTi surface after (a) 30 minutes, (b) 60 minutes and (c) 90 minutes anodization process.

Similarly, *Raja et al.* [18] showed that the anodizing time which was necessary for the formation of the nanotubular oxide layer on cpTi surface in the electrolyte with fluoride ions was 50 minutes. It was shown that by increasing the anodizing time, the nanotube diameter increases too and homogeneous distribution of the nanotubes is formed. On the contrary, by increasing the concentration of fluoride ions, the nanotube diameter decreases and oxide layer degrades [19]. *Gong et al.* [20] formed nanotubular oxide layer on the cpTi surface in HF electrolyte at different voltages and during different time periods. They concluded that the nanotubular oxide layer could be formed under voltages from 10 to 40 V, while the anodizing time influenced the diameter and degradation of nanotubes. *Beranek et al.* [21] formed nanotubular oxide layer in 1M  $H_2SO_4 + 0.15$  wt. % HF during anodizing times of 24 h, and showed that limited thickness was 580 nm after the anodizing time of 12 h. On the contrary, *Ghicov et al.* [22] showed that increasing the anodizing time from 5 minutes to 40 minutes, the nanotube length increases from 2.34  $\mu m$  to 4.07  $\mu m$  in  $(NH_4)H_2PO_4 + 0.5$  wt%  $NH_4F$  electrolyte.

Table 2 shows an average chemical composition of five selected positions on the nanotubular surface. Fig. 5 presents characteristic spectra of elements obtained by the SEM/EDS technique. The obtained results indicate the presence of Ti and O in value of 57.05% and 42.74%, respectively. One of the five analysed positions showed the presence of Na and P in the amount of 0.34% and 0.26%, respectively. The presence of Na and P is detected as a consequence of residual electrolyte, which was used in anodization process.

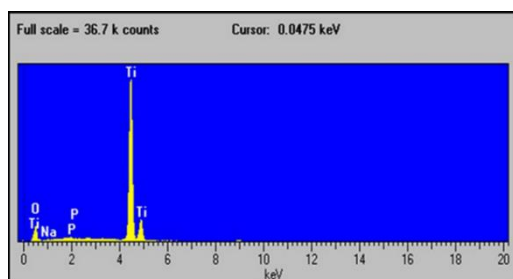


Fig. 5. The elements spectra of the nanotubular surface.

Table 2. EDS analysis of the nanotubes (in wt %)

|    |       |
|----|-------|
| Ti | 57.05 |
| O  | 42.74 |
| Na | 0.34  |
| P  | 0.26  |

### The Characterisation of surface using Atomic Force Microscopy

The AFM was used to analyse the surface topography as shown in Fig. 6. Images clearly indicate that the anodization process lead to creation of the rough topography surface. Typical surface roughness of titanium after nanostructured modification is in the range of 10 to 100 nm [23, 24]. The surfaces topographies of examined materials present areas with pronounced peaks / valleys. The roughness of UFG cpTi is 5.33 nm, while UFG cpTi after anodization process has roughness of 15.73 nm, which indicates that the anodization process increases three times the roughness of the surface. It was shown that the nanostructure modification of the surface influences the adhesion, spread and growth

of human cells. The formation of the  $\text{TiO}_2$  nanoporous surface on the titanium has a positive influence on the rate of human cell proliferation compared to titanium without the  $\text{TiO}_2$  nanoporous surface [25].

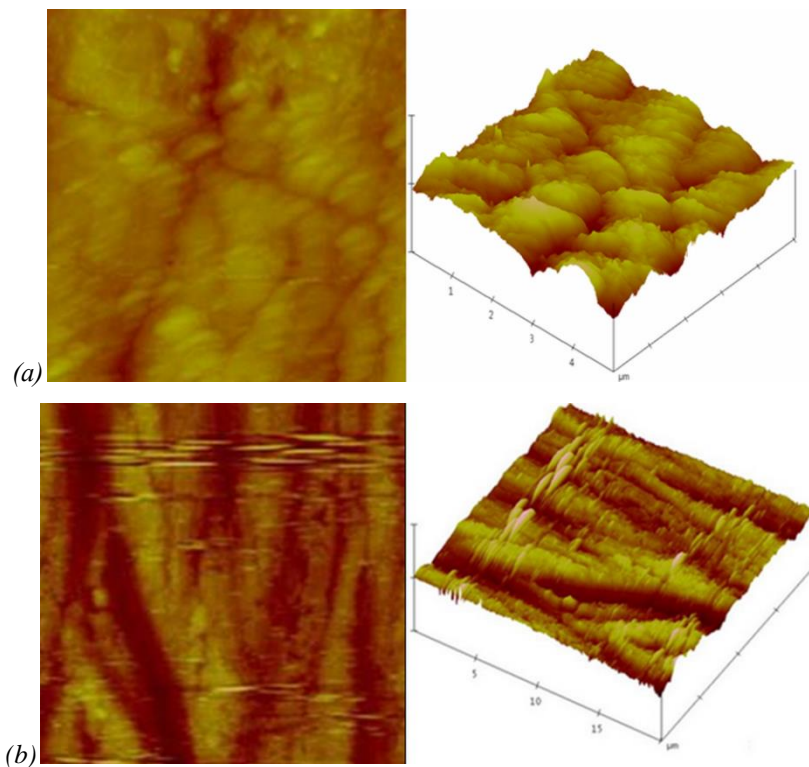


Fig. 6. AFM images of (a) the UFG cpTi and (10x10x0.7) (b) the nanotubular oxide layer of UFG cpTi prepared in 1M  $\text{H}_3\text{PO}_4$  + 0.5 wt.% NaF solution at 25V after anodizing time of 60 minutes (20x20x3).

### Mechanical characterization

Maximum mean values of load on UFG cpTi was approximately 375 mN for a displacement of 2000 nm [26], while maximum mean values of the load on UFG cpTi after anodization process was 2.25 mN for a displacement of 300 nm. The loading-displacement curve obtained during nanoindentation test is presented in Fig. 7. Permanent (plastic) deformation of examined material was confirmed by the difference between the loading part and unloading part on the diagrams. The mean values of mechanical characteristics of the surface, nanohardness and modulus of elasticity, obtained from the nanoindentation test after the ten measurements, are presented in Table 3.

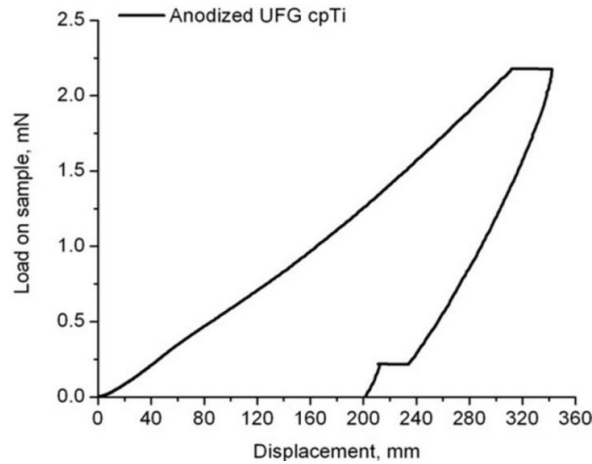


Fig. 7. Loading-displacement curve for UFG cpTi after anodizing time of 60 minutes.

Table 3. The values of mechanical properties for UFG cpTi [25] and anodized UFG cpTi.

| Materials                     | UFG cpTi | Anodized UFG cpTi |
|-------------------------------|----------|-------------------|
| Displacement, nm              | 2000     | 300               |
| Modulus of elasticity, E, GPa | 104.56   | 16.157            |
| Nanohardness, H, GPa          | 3.54     | 0.674             |
| Nanohardness, H, HV           | 361      | 68.73             |

The results show decreasing values of nanohardness after anodization process. As can be seen in Table 3, the nanohardness value of the UFG cpTi decreases significantly after anodization processing, from 361 HV in the initial state to 68.73 HV. Moreover, the results show that the modulus of elasticity is lower after anodization process. As can be seen in Table 3, the modulus of elasticity value of UFG cpTi decreases significantly after anodization processing, from 104.56 GPa in the initial state to 16.157 GPa. The lower value of modulus of elasticity indicates that UFG cpTi after anodization process is a more acceptable material for the implant. This lower value of modulus of elasticity and closer to that of a bone (10-30 GPa) [27] is one of the important factors in accepting the implant from the surrounding bone [28]. These results are in agreement with examination of Crawford's group [29] who confirmed decreasing of modulus of elasticity after anodizing time of 0.25 h and 4 h. They obtained the values for modulus of elasticity for cpTi in the range of 4.6 GPa to 7.2 GPa for the anodization process after 4 h and 0.25 h, respectively. It was shown that the anodization process after 2 h decreases the modulus of elasticity of cpTi in the range of 36-43 GPa. Moreover, increasing anodizing time leads to enhanced thickness of the nanotubular oxide layer, which in turn leads to a decrease in values for modulus elasticity [30].

## Conclusion

Results show that electrochemical anodization is a suitable process for obtaining nanotubular oxide layer on the ultrafine-grained titanium. The electrochemical anodization was performed on the ultrafine-grained titanium in the 1M H<sub>3</sub>PO<sub>4</sub> + 0.5 wt. % NaF electrolyte during anodizing times of 30, 60 and 90 minutes. The SEM image showed that only the anodization process after 60 minutes led to the formation of a nanotubular oxide layer. The nanotubes had a homogenous morphology with an average diameter of 100 nm, while the thicknesses of the nanotube walls were approximately 30 nm. The analysing surface topography indicates that anodization process increases roughness of the surface. Nanoindentation tests show that anodized UFG cpTi had a lower modulus of elasticity and nanohardness, which make them more acceptable as biomaterials.

## Acknowledgements

The authors acknowledge the support of the Ministry of Education, Science and Technological Development of the Republic of Serbia through the project ON 174004 and III 45019. Also the authors gratefully acknowledge prof. dr Reinhard Pippan and dr Anton Hohenwarter from Erich Schmid Institute of Material Science, Leoben - Austria, for the preparation of UFG samples, prof. dr Goran Stojanović from the University of Novi Sad, Faculty for Technical Science for his help in nanoindentation testing and dr Sanja Stevanović from University of Belgrade, Institute for Chemistry, Technology and Metallurgy for her help in AFM analysing.

## References

- [1] D. Duraccio, F. Mussano, M. Faga: *Biomaterials*, *J Mater Sci*, 50 (2015) 4779–4812.
- [2] M. Esposito, V. Worthington, P. Thomsen, P. Coulthard: *Coch Data Syst Rev*, 2003: CD003815.
- [3] G. Hille: *J Mater*, 1 (1966) 373–383.
- [4] I. Brånemark, *Introduction to osseointegration*, Quintessence, Chicago, 1985.
- [5] R. Roach: *Dent Clin North Am*, 51 (2007) 603–627.
- [6] R. Valiev, I. Semenova, E. Jakushina, V. Latysh, H. Rack, T. Lowe, J. Petruželka, L. Dluhoš, D. Hrušák, J. Sochová: *Mater Sci For*, 584-586 (2008) 49-54.
- [7] I. Dimić, I. Cvijović-Alagić, A. Hohenwarter, R. Pippan, V. Kojić, J. Bajat, M. Rakin: *J Biomed Mater Res B: App Biomater*, 106 (2018) 1097-1107.
- [8] H. Yilmazer, M. Niinomi, M. Nakai, K. Cho, J. Hieda, Y. Todaka, T. Miyazaki: *Mater Sci and Eng C*, 33 (2013) 2499–2507.
- [9] K. Edalati, Z. Horita: *Mater Sci & Eng, A* 652 (2016) 325–352.
- [10] M. Diamanti, M. Pedferri: *Corr Sci*, 49 (2007) 939–948.
- [11] L. Wang, M. Jin, Y. Zheng, Y. Guan, X. Lu, J. Luo: *Int J Nanomed*, 9 (2014) 4421-4435.
- [12] D. Barjaktarević, I. Cvijović-Alagić, I. Dimić, V. Đokić, M. Rakin: *Metall Mater Eng*, 22 (2016) 129-143.
- [13] X. Feng, J. Macak, S. Albu, P. Schmuki: *Acta Biomater*, 4 (2008) 318–323.
- [14] L. Taveira, J. Macák, H. Tsuchiya, L. Dick, P. Schmukib: *J of Electro Soc*, 10 (2005) B405-B410.
- [15] N. El-Wasefy, I. Hammouda, A. Habib, G. El-Awady, H. Marzook: *Clin Oral Impl Res*, 25 (2014) e1-e9.

- [16] L. Wang, M. Jin, Y. Zheng, Y. Guan, X. Lu, J. Luo: *Inter J Nanomed*, 9 (2014) 4421–4435.
- [17] A. Fischer-Cripps, *Nanoindentation*. 2nd ed. New York: Springer; 2004.
- [18] K. Raja, M. Misra, K. Paramguru: *Electroch Acta*, 51 (2005) 154–165.
- [19] S. Chatterjee, M. Ginzberg, B. Gersten: In: *MRS Proceedings*, 2006, p. 951.
- [20] D. Gong, C. Grimes, O. Varghese, W. Hu, R. Singh, Z. Chen, E. Dickey: *J Mater Res*, 16 (2001) 3331-3334.
- [21] R. Beranek, H. Hildebrand, P. Schmuki: *Electrochem Solid-State Lett*, 6 (2003) B12.
- [22] A. Ghicov, H. Tsuchiya, J. Macak, P. Schmuki: *Electroch Commun*, 7 (2005) 505–509.
- [23] C. Larsson, P. Thomsen, J. Lausmaa, M. Rodahl, B. Kasemo, L. Ericson: *Biomater*, 15 (1994) 1062 -1074.
- [24] M. Ask, U. Rolander, J. Lausmaa, B. Kasemo: *J Mater Res*, 5 (1990) 1662 – 1667.
- [25] A. Novaes, S. Scombatti, R. Martins, K. Pereira, G. Iezzi, A. Piattelli: *Braz Dent J*, 21 (2010) 471-481.
- [26] D. Barjaktarević, M. Rakin, B. Međo, V. Đokić: *Proceedings of TEAM 2018*, 2018, 117-122, <http://iim.ftn.uns.ac.rs/team2018/topics.html>.
- [27] Y. Bai, Y. Deng, Y. Zheng, Y. Li, R. Zhang, Y. Lv, Q. Zhao, S. Wei: *Mater Sci and Eng C*, 59 (2016) 565–576.
- [28] A. Ossowska, S. Sobieszczyk, M. Supernak, A. Zielinski: *Sur & Coat Techn*, 258 (2014) 1239-1248.
- [29] G. Crawford, N. Chawla, J. Houston: *J Mech Behav Biomed Mater*, 2(2009) 580 - 587.
- [30] G. Crawford, N. Chawla, K. Das, S. Bose, A. Bandyopadhyay: *Acta Biomater*, 3 (2007) 359-367.



Creative Commons License

This work is licensed under a Creative Commons Attribution 4.0 International License.